

Macrophage ferroportin is essential for stromal cell proliferation in wound healing

Stefania Recalcati,^{1#} Elena Gammella,^{1#} Paolo Buratti,¹ Andrea Doni,² Achille Anselmo,² Massimo Locati^{2,3} and Gaetano Cairo¹

¹Department of Biomedical Sciences for Health, University of Milan; ²Humanitas Clinical and Research Center, Rozzano and ³Department of Medical Biotechnologies and Translational Medicine, University of Milan, Italy

SR and EG contributed equally to this work

©2019 Ferrata Storti Foundation. This is an open-access paper. doi:10.3324/haematol.2018.197517

Received: May 14, 2018.

Accepted: August 14, 2018.

Pre-published: August 16, 2018.

Correspondence: gaetano.cairo@unimi.it or massimo.locati@humanitasresearch.it or massimo.locati@unimi.it

SUPPLEMENTAL METHODS

Animals.

Mice carrying a floxed Fpn allele ($Fpn^{fl/fl}$) (1), generously provided by Dr Nancy Andrews (Duke University), were bred to mice expressing Cre under the control of the LysM promoter in the C57BL/6J background (2) (backcrossed for 11 generations) in order to generate mice with specific FPN-macrophage inactivation ($Fpn1^{fl/fl}LysCre^{+/-}$). $Fpn1^{fl/fl}LysCre^{+/-}$ mice were cohoused with littermates $Fpn1^{fl/fl}LysCre^{-/-}$ mice in individually ventilated cages in a specific pathogen-free animal facility at Humanitas Clinical and Research Center. $Fpn1^{fl/fl}LysCre^{+/-}$ mice were born in mendelian ratios, reproduced normally and did not show significant differences in body weight compared to control floxed littermates ($Fpn1^{fl/fl}LysCre^{-/-}$). Efficient FPN deletion in macrophages was demonstrated in bone marrow derived macrophages (BMDM) and in macrophages derived from peritoneal exudate cells (PEC). Moreover, the functional relevance was shown by the increased iron accumulation revealed in spleen and liver macrophages (Fig. S1). Mice were usually maintained with normal diet (157 ppm iron content). All pups were weaned at 3 weeks of age. When appropriate, dams and pups were provided with an iron-deficient diet (9 ppm iron content; ssniff® EF R/M iron-deficient experimental diet, Charles River). Only some groups were given an iron-deficient diet for 11 weeks after birth, as indicated. Alopecia was quantified as follows: 100% = complete hair loss on the trunk; 50% = initial thin dorsal pelage; 0% = normal coat hair.

Primary cell cultures.

BMDM were generated as previously reported (3). Briefly, bone marrow aspirates from femura of 8- to 12-week old mice were harvested and flushed out with Iscove modified Dulbecco medium (IMDM), 10% fetal calf serum (FCS) (Euroclone, Pero, Italy). After addition of ACK lysis buffer (Thermo Scientific, Milano, Italy) for red cells lysis, bone marrow cells were left to adhere overnight. Non-adherent cells were centrifuged and suspended at 0.5×10^6 cells/mL in complete bone

marrow macrophage medium (IMDM, 10% FCS, 150 μ M MTG, 10 ng/mL M-CSF) and cultured for 7 days. BMDM were stimulated by changing the medium to IMDM, 10% FCS, 150 μ M MTG, 1% P/S, 1% L-glutamine, and 100 ng/mL LPS plus 20 ng/mL IFN γ or 20 ng/mL IL-4 for 24 h. PEC were recovered from the peritoneal cavity of mice injected with 1 ml of 3% (wt/vol) dithioglycolate (Difco, BD Biosciences, Milano, Italy) as previously reported (4). Briefly, 4-5 days after treatment, peritoneal cells were recovered in 5 ml of saline, centrifuged at 400 x g for 8 minutes, and cultured for 1 h in RPMI. After washing with PBS, adherent macrophages were cultured in RPMI containing 10% FCS.

Immunoblot analysis.

For the preparation of membrane extracts, BMDM and PEC were homogenized in 10 mM Tris-HCl, pH 7.0, 1 mM MgCl₂ and the postnuclear supernatant fraction obtained by centrifugation at 2000g for 10 minutes was ultracentrifuged at 150000g for 20 minutes to pellet crude membrane fractions (5). Equal amounts of protein extracts were electrophoresed in acrylamide-SDS gels, electroblotted to Hybond membranes (Amersham Biosciences, Euroclone) and incubated with antibodies against FPN (1:250; Alpha Diagnostic, DBA, Segrate, Italy). After incubation with the secondary antibody, the protein was detected by means of chemiluminescence (ECL Plus; Amersham Biosciences, Euroclone). Signals were detected using the ChemiDoc Touch system (BioRad, Segrate, Italy) and signal intensity was quantified using ImageLab 5.2.1 software with the values being calculated after normalisation to amido black-stained proteins.

Histology and assessment of tissue sections.

The mice were received as whole body fixed. Organs and tissues were examined for gross lesions, trimmed after complete fixation and processed for paraffin blocks embedding. From each mouse 5 blocks/sections were obtained containing a scheduled list of organs/tissues. For histopathological analysis, 4 μ m-thick tissue sections obtained from the paraffin blocks were stained with hematoxylin and eosin. For iron detection, 4 μ m sections from each sample were stained with Perls' Prussian blue

stain and semi-quantitatively evaluated under a light microscope as follows: 0 = absence of iron laden cells; 1 = rare iron laden cells; 2 = small number of iron laden cells; 3 = moderate numbers of iron laden cells; 4 = large number of iron laden cells.

Skin wound healing model.

To generate a punch wound, the back of anesthetized mice was shaved and exposed skin was cleaned with 70% ethanol. A full-thickness wound was created with a disposable 8-mm-diam biopsy punch by excising the skin and the underlying *panniculus carnosus* (6). Gentamicin was immediately applied and upon histological analysis no gross infection was apparent through day 14. Wound sites of each mouse were digitally photographed and measured every day in the course of wound healing. The edges of the wounds were daily traced onto a transparency and the areas of open wounds were calculated using ImageJ software (National Institutes of Health). Changes of wound area over time were expressed as percentage of the initial wound areas. The animals were sacrificed at different times and skin biopsies were fixed with 4% paraformaldehyde, and embedded in paraffin or dehydrated with a sucrose gradient and embedded in OCT compound (Diapath, Bergamo, Italy) and stored at -80°C for histology or confocal microscopy analysis, respectively. Alternatively, skin biopsies were directly used for mRNA extraction, FACS and ELISA.

Blood analysis.

Blood was collected by cheek puncture. Hemoglobin, and hematocrit were measured using the Hemo Vet Instrument (Infratec, Portomaggiore, Italy) following manufacturer's instructions; red blood cells, MCV and MHC by using the Sysmex KX-21 automated analyser (Sysmex Italy Cornaredo).

Serum iron determination: blood was collected by cardiac puncture and serum iron was measured using standard laboratory procedures. Transferrin was measured using the mouse transferrin ELISA kit (ab157724, Abcam DBA, Italy) and transferrin saturation was calculated as serum iron concentration ($\mu\text{g/dL}$) \times 100 / [serum transferrin (mg/dL) \times 1.42].

ELISA assay.

Whole wounds were collected at 2, 7, and 12 days after wounding and homogenized in 50 mM Tris-HCl, pH 7.5, containing 2 mM EGTA, 1 mM PMSF, 100 KU aprotinin, 1% Triton X-100 (all from Sigma-Aldrich, Milano, Italy), and complete protease inhibitor cocktail (Roche, Monza, Italy). Total proteins were measured by DC Protein Assay, according to manufacturer's instructions (Bio-Rad Laboratories, Segrate, Italy). Cytokine levels were measured in accordance with the manufacturer's instructions (R&D Systems, Space, Milano, Italy). Hepcidin levels were measured using a specific kit (Cloud-Clone Co, Houston, TX, USA) according to the manufacturer's instructions.

Flow cytometry and cell sorting.

A single-cell suspension of wounded skin was generated by cutting samples into small pieces and digestion in PBS (pH 7.4) supplemented with collagenase type I (1 mg/ml; Sigma-Aldrich) and hyaluronidase (125 U/ml; Sigma-Aldrich) at 37°C for 1 h, twice. Finally, a single-cell suspension was obtained by mechanical separation followed by 100 µm filtration and erythrocyte lysis in 0.15 M NH₄Cl, 10 nM KHCO₃, 1 nM Na₄EDTA, pH 7.2. The following fluorophore-conjugated antibodies were used for immunophenotyping and intracellular staining: anti-mouse CD45 BV605TM (#30-F11; BD Biosciences); anti-mouse Ly6G PE-CF594TM (#1A8; BD Biosciences); anti-mouse Ly6C BV421TM (#AL-21; BD Biosciences); anti-mouse CD11b PerCP-Cy7TM5.5 (#M1/70; BD Biosciences); anti-mouse F4/80 PE-Cy7TM (#BM8; BioLegend, Campoverde, Milano, Italy); anti-mouse CD3 APC (#145-2C11 eBioScience, Thermo Fisher); anti mouse MHCII BV711 (#M5/114 BD Biosciences); CD206 PE (#C068C2 BioLegend); CD195 FITC (CCR3) (#J073E5 BioLegend). Dead cells exclusion was performed using LIVE /DEAD fixable Aqua dead cell stain kit (Life Technologies, Thermo Fisher) at room temperature for 15 minutes following the manufacturer instructions. All gated regions were restrictively defined using Fluorescence Minus One as negative control. Stained cells were analysed and/or sorted using FACS LSR Fortessa flow cytometer (BD

Biosciences) or BD FACSAria III cell sorter (BD Biosciences). Diva software (Version 8.0.1) (BD Biosciences) was used for data acquisition and analysis. The purity of sorted cells was $\geq 98\%$.

Confocal microscopy.

Cryostat sections were incubated in 5% of normal goat (Dako, Milano, Italy) or donkey (Sigma-Aldrich) serum, 2% BSA, 0.1% Triton X-100 (Sigma-Aldrich) in PBS with calcium and magnesium chloride (PBS²⁺) pH 7.4 for 1 h at room temperature. Specimens were incubated with the following primary antibodies for 2 h at room temperature: rat monoclonal anti-PDGFR (#4C54, 2 $\mu\text{g/ml}$; Cell Sciences); rabbit polyclonal anti-collagen I (4 $\mu\text{g/ml}$; AbCam, Euroclone); Cy3-conjugated mouse monoclonal anti- α -SMA (#1A4, 2 $\mu\text{g/ml}$; Sigma-Aldrich); rabbit monoclonal anti-Ki67 (#D3B5, 1:400; Cell Signaling Technology, Euroclone); rabbit monoclonal anti-TfR1 (0.5 $\mu\text{g/ml}$; Invitrogen); rat anti-F4/80 (#T45-2342, 1:500, BD Biosciences); rat monoclonal anti-CD31 (#MEC 13.3, 1 $\mu\text{g/ml}$; BD Biosciences); rabbit polyclonal anti-Lyve-1 (2 $\mu\text{g/ml}$; AbCam, Euroclone), rabbit polyclonal anti mouse ferritin H subunit (Z17, 1:200) and L subunit (E17, 1:200), both kindly provided by Dr. Maura Poli (University of Brescia, Italy). Sections were then incubated for 1 h with Alexa Fluor[®] (488, 594, 647)-conjugated species-specific cross-adsorbed detection antibodies (Thermo Fisher Molecular Probes). For DNA detection, DAPI (300 nM; Thermo Fisher-Molecular Probes) was used. After each step, sections were washed with PBS²⁺ pH 7.4 containing 0.01% (vol/vol) Tween 20. Sections were mounted with the antifade medium FluorPreserve Reagent (EMD Millipore, Vimodrone, Italy) and analyzed with an Olympus Fluoview FV1000 laser scanning confocal microscope (Olimpus, Segrate, Italy). Immunoreactive areas were measured using the computer-assisted digital image processing software Image-Pro Plus (version 7.0; Media Cybernetics). The total stained area was automatically selected on the basis of RGB color segmentation and results are expressed as mean percentage of the immunoreactive area \pm SEM.

Quantitative real-time polymerase chain reaction (qRT-PCR).

Total RNA isolated from liver, spleen, normal skin, wounds, bone marrow, PEC or BMDM using TRI reagent® (Sigma-Aldrich) was reverse transcribed into cDNA with Proto Script M-MuLV First Strand cDNA Synthesis Kit (New England Biolabs, Euroclone) and the obtained cDNA served as a template for Real-Time PCR, based on the TaqMan methodology (Life Technologies, Thermo Fisher). Thermal cycling parameters were 40 cycle at 95° C for 15s and 60° C for 1 min. Each sample was amplified in triplicate using the primers reported in Table S2 (Applied Biosystems, Thermo Fisher) and the amount of RNA was calculated using the $2^{-\Delta C_t}$ method. Results were normalized to 18S RNA and the housekeeping gene ribosomal protein, large, P0 (RPLPO) with similar results (in the figures only 18S RNA is shown).

SUPPLEMENTAL TABLES

Supplemental Table 1. Haematologic parameters of Fpn1^{fl/fl}LysCre^{-/-} and Fpn1^{fl/fl}LysCre^{+/-} mice.

	Fpn ^{fl/fl} LysCre ^{-/-}		Fpn ^{fl/fl} LysCre ^{+/-}		Fpn ^{fl/fl} LysCre ^{-/-}		Fpn ^{fl/fl} LysCre ^{+/-}	
	3 weeks	6 weeks	3 weeks	6 weeks	3 weeks	6 weeks	3 weeks	6 weeks
	Normal diet				Iron deficient diet			
Red blood cells (x10 ⁶ /mm ³)	9.2±0.2	10.4±0.9*	7.7±0.5**	9.8±0.9 ^{ooo}	6.9±0.4	9.5±0.7***	6.1±0.4	9.4±0.5 ^{ooo}
MCV (fL)	44±2.6	46±3.5	43±3.1	45±2.1	36±1.9	44.8±3.2***	32.5±1.9	44±2.5 ^{ooo}
MCH (pg)	14±1.9	15±2.1	13.5±1.9	15±2.9	12.5±0.4	15±0.6***	12±0.4	15±0.7 ^{ooo}

Data are mean ±SEM, n= 6 for each group. *** p< 0.0001, ** p< 0.001, * p< 0.01 vs 3-week-old Fpn1^{fl/fl}LysCre^{-/-} mice; ^{ooo} p< 0.0001 vs 3-week-old Fpn1^{fl/fl}LysCre^{+/-} mice. MCV indicates mean corpuscular volume, MCH mean corpuscular haemoglobin.

Supplemental Table 2. Wound healing histological grading.

The grading is based on separate evaluation of distinct features of wound healing process.

Response	Cell type	Score			
		0	1	2	3
Re-epithelialization	Migration of epidermal cells from the edges to the center of the wound	Absent	Mild (<50% of the wound)	Moderate (>50% of the wound, but still incomplete)	Complete
Granulation tissue	<u>Immature</u> : loose granulation tissue composed of fibroblasts and macrophages with emerging disorganized vessels	Absent	Wound bed partially covered with granulation tissue	Thin granulation tissue over the whole bed	Thick granulation tissue over the whole bed
	<u>Mature</u> : fibroblasts, initial collagen deposition (loose collagen fibers), perpendicular arranged blood vessels	Absent	Wound bed partially covered with granulation tissue	Thin granulation tissue over the whole bed	Thick granulation tissue over the whole bed
Fibrosis*	More abundant and regular collagen deposition (dense collagen fibers), fewer fibroblast/fibrocytes and vessels	Absent	Mild amount of dense collagen fibers between fibroblast	Moderate amount of dense collagen fibers between fibroblast	Large amount of dense collagen fibers between fibroblast
Inflammation	Mononuclear cells Infiltrate	Absent	Mild	Moderate	Heavy
	Granulocyte infiltrate	Absent	Mild	Moderate	Heavy

* Transition from mature granulation tissue and fibrosis was occurring at late time-point (dpi 12). In this case, the amount of deposition of dense extracellular matrix, i.e. collagen fibers, was evaluated.

Supplemental Table 3. Primers for qRT-PCR.

Gene	TaqMan gene expression assay ID
TfR1	Mm00441941_m1
Fpn	Mm01254820_m1
Rn18s	Mm03928990_g1
FtH	Mm04336019_g1
Fam132b	Mm00557748_m1
Arg1	Mm00475988_m1
TNF α	Mm00443260_g1
iNOS	Mm00440502_m1
Hepcidin	Mm04231240_s1
CD163	Mm00474091_m1
YM1	Mm00657889_mH

REFERENCES

1. Donovan A, Lima CA, Pinkus JL, Pinkus GS, Zon LI, Robine S, et al. The iron exporter ferroportin/Slc40a1 is essential for iron homeostasis. *Cell Metab.* 2005 Mar;1(3):191-200.
2. Clausen BE, Burkhardt C, Reith W, Renkawitz R, Förster I. Conditional gene targeting in macrophages and granulocytes using LysMcre mice. *Transgenic Res.* 1999 Aug;8(4):265-77.
3. Weischenfeldt J, Porse B. Bone Marrow-Derived Macrophages (BMM): Isolation and Applications. *CSH Protoc.* 2008 Dec;2008:pdb.prot5080.
4. Zhang X, Goncalves R, Mosser DM. The isolation and characterization of murine macrophages. *Curr Protoc Immunol.* 2008 Nov;Chapter 14:Unit 14.1.
5. Delaby C, Pilard N, Gonçalves AS, Beaumont C, Canonne-Hergaux F. Presence of the iron exporter ferroportin at the plasma membrane of macrophages is enhanced by iron loading and down-regulated by hepcidin. *Blood.* 2005 Dec;106(12):3979-84.
6. Nakayama Y, Kon S, Kurotaki D, Morimoto J, Matsui Y, Uede T. Blockade of interaction of alpha9 integrin with its ligands hinders the formation of granulation in cutaneous wound healing. *Lab Invest.* 2010 Jun;90(6):881-94.

SUPPLEMENTAL FIGURE

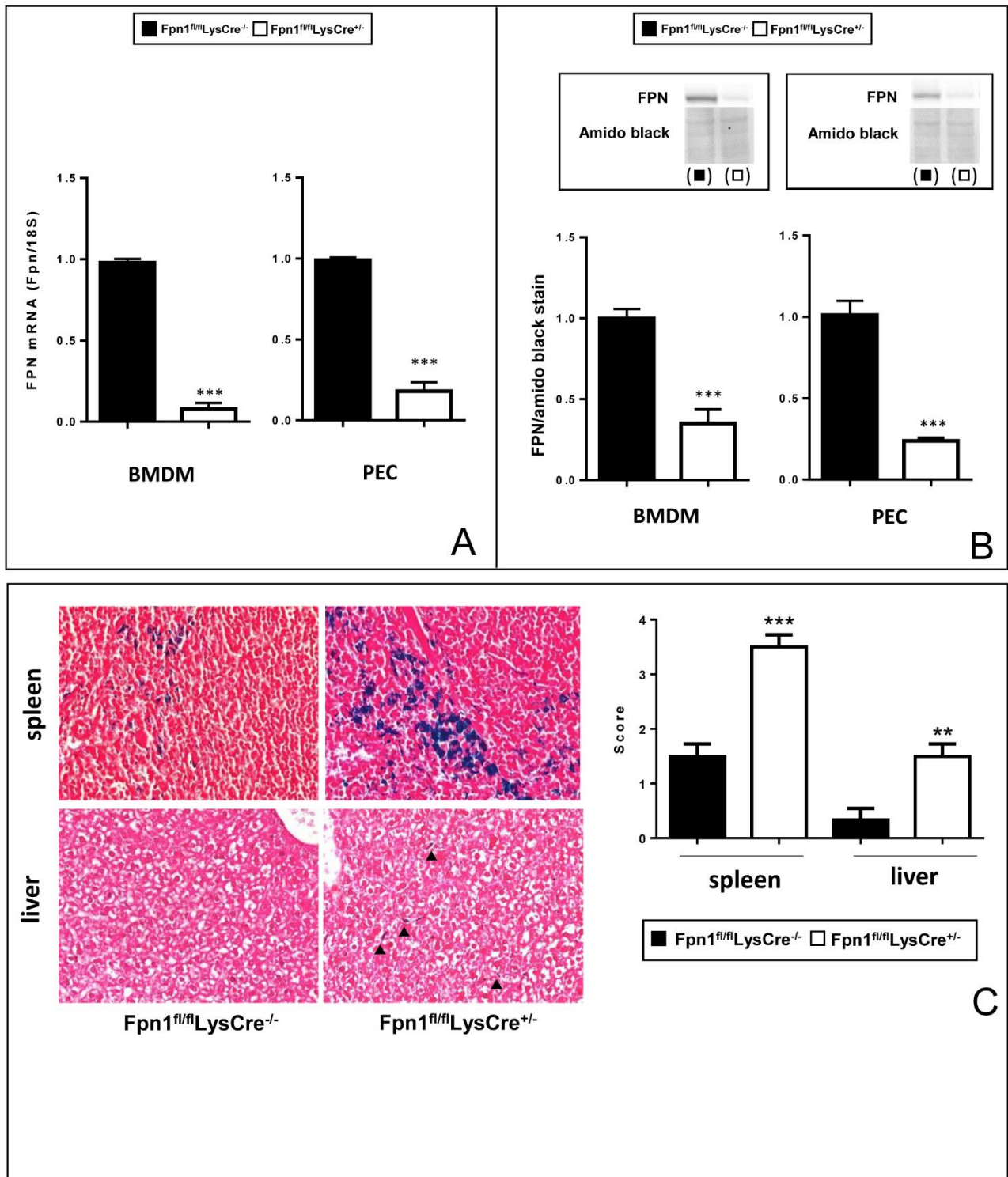


Figure S1. FPN deletion and iron accumulation in macrophages of *Fpn1^{fl/fl}LysCre^{+/-}* mice.

(A) FPN mRNA levels in bone marrow derived macrophages (BMDM) and peritoneal exudate cells (PEC) from *Fpn1^{fl/fl}LysCre^{-/-}* and *Fpn1^{fl/fl}LysCre^{+/-}* mice were measured by quantitative RT-PCR; results were normalized to the housekeeping gene 18S RNA (mean ± SEM of n=50 mice for each group; *** p < 0.0001).

(B) Representative blots and densitometric quantitation (mean \pm SEM of n=20 mice for each group; *** p< 0.0001 vs Fpn1^{fl/fl}LysCre^{-/-}) of immunoblot analysis of membrane FPN in BMDM and PEC from Fpn1^{fl/fl}LysCre^{-/-} and Fpn1^{fl/fl}LysCre^{+/-} mice. The blots were stained with amido black to assess equal protein loading. (C) Representative histology of Perls' Prussian blue iron staining in paraffin sections of spleen and liver from Fpn1^{fl/fl}LysCre^{-/-} and Fpn1^{fl/fl}LysCre^{+/-} mice. Arrowheads indicate iron-stained cells in the liver. A semi-quantitative evaluation of Perls' iron staining in spleen and liver (performed as reported in Materials and Methods) is also shown. n = 6 for each group. *** p< 0.0001, ** p< 0.001 vs Fpn1^{fl/fl}LysCre^{-/-}. Magnification: 40X.

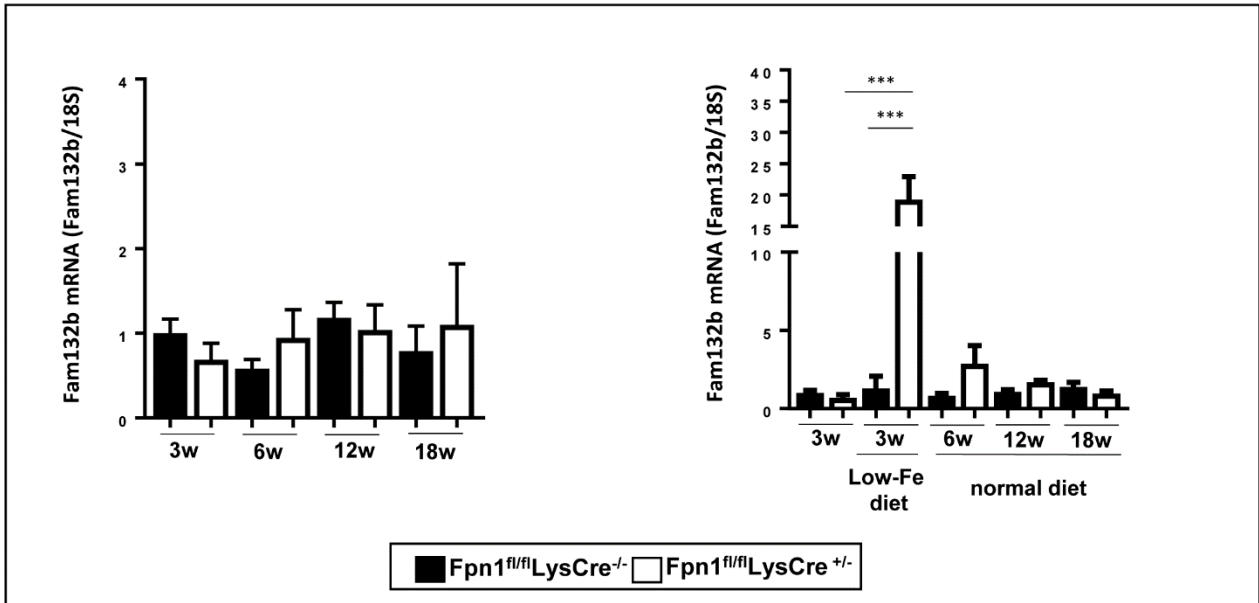


Figure S2. Erythroferrone expression in bone marrow.

Erythroferrone (Fam132b) mRNA levels in the bone marrow of mice fed the normal or the iron-deficient diet at different age. mRNA levels were measured by quantitative RT-PCR and normalized to the housekeeping gene 18S RNA. Data are presented as mean \pm SEM. n = 10 mice for each group. *** p < 0.0001.

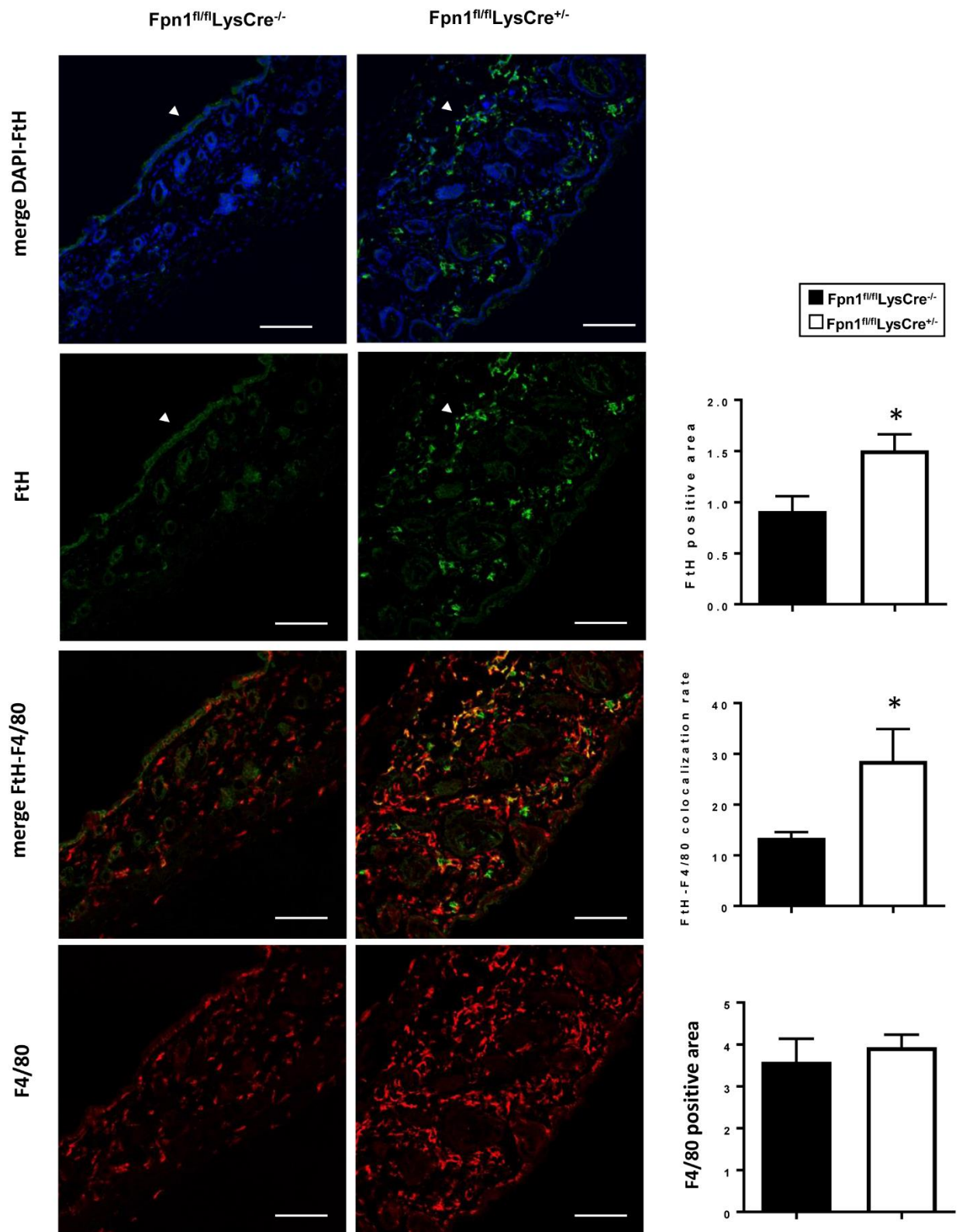


Figure S3. Ferritin expression shows macrophage iron accumulation and epithelial iron deficiency in cutaneous hair follicles of $Fpn1^{fl/fl}LysCre^{+/-}$ mice.

Expression and localization of ferritin H subunit (FtH) and F4/80 in cutaneous tissue of $Fpn1^{fl/fl}LysCre^{-/-}$ and $Fpn1^{fl/fl}LysCre^{+/-}$ mice was assessed by confocal microscopy. Representative confocal microscopy images and

the relative quantification for merge signals, FtH and F4/80 (5-9 field of vision/mouse, 3 mice/group) are shown. * $p < 0.01$ vs $Fpn1^{fl/fl}LysCre^{-/-}$. The top panel shows confocal images of FtH and DAPI counterstain. Arrowheads indicate FtH expression in epithelial cells of $Fpn1^{fl/fl}LysCre^{-/-}$ mice and macrophages of $Fpn1^{fl/fl}LysCre^{+/-}$ mice. Bars: 100 μ m. Magnification: 40X.

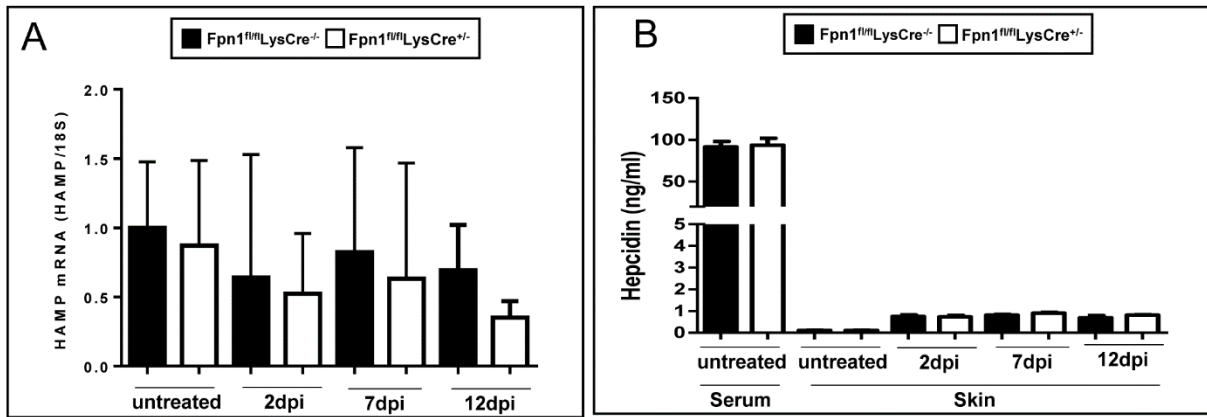


Figure S4. Liver hepcidin expression and hepcidin levels in skin wounds are not altered in *Fpn1^{fl/fl}LysCre^{+/-}* mice.

(A) Hepcidin (HAMP) mRNA levels in liver of mice untreated and at different days post injury (dpi) were measured by quantitative RT-PCR and normalized to the housekeeping gene 18S RNA. Data are presented as mean \pm SEM of n=12 mice for each group. (B) Hepcidin protein levels in serum and wound lysates at different dpi were measured by ELISA. n = 4 and 12 for each group, respectively.

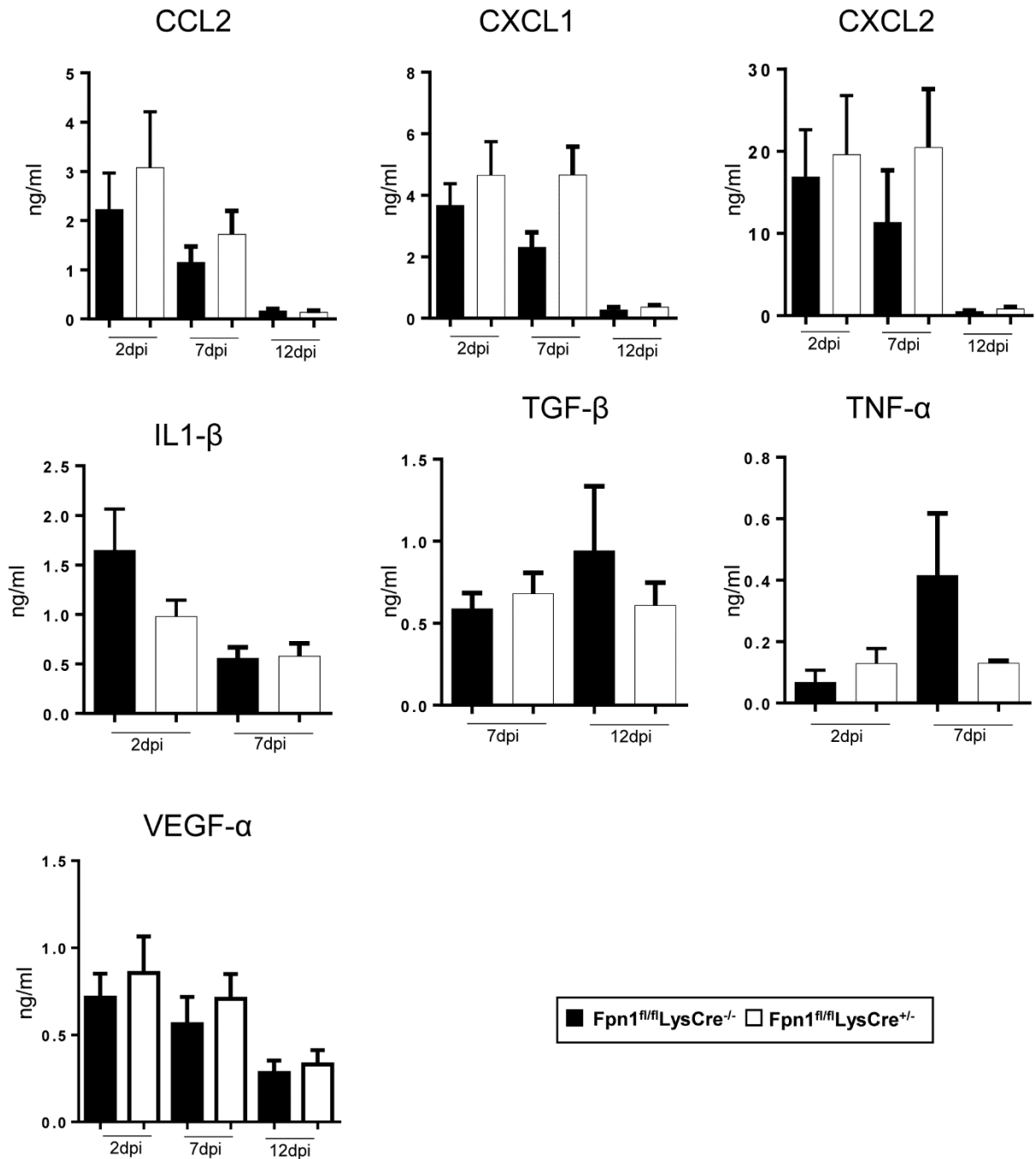


Figure S5. Cytokines and growth factors levels in skin wound are not altered in $Fpn1^{fl/fl}LysCre^{+/-}$ mice.

CCL2, CXCL1, CXCL2, IL-1 β , TGF β , TNF α and VEGF α protein levels in wound lysates were assessed by ELISA at different times after skin injury. At the time points not shown, the levels of the respective cytokine were below the detection limit of the assay. The histograms show the mean \pm SEM. n = 10 mice for each group.